

# Fluid dynamical aspects of the levitation-melting process

By A. D. SNEYD

University of Waikato, Hamilton, New Zealand

AND H. K. MOFFATT

Department of Applied Mathematics and Theoretical Physics,  
Silver Street, Cambridge

(Received 28 May 1981)

When a piece of metal is placed above a coil carrying a high frequency current, the induced surface currents in the metal can provide a Lorentz force which can support it against gravity; at the same time the heat produced by Joule dissipation can melt the metal. This is the process of 'levitation melting', which is a well-established technique in fundamental work in physical and chemical metallurgy. Most theoretical studies of magnetic levitation have dealt only with solid conductors and so have avoided the interesting questions of interaction between the free surface, the magnetic field and the internal flow. These fluid dynamical aspects of the process are studied in this paper.

A particular configuration that is studied in detail is a cylinder levitated by two equal parallel currents in phase; this is conceived as part of a toroidal configuration which avoids a difficulty of conventional configurations, viz the leakage of fluid through the 'magnetic hole' at a point on the metal surface where the surface tangential magnetic field vanishes. The equilibrium and stability of the solid circular cylinder is first considered; then the dynamics of the surface film when melting begins; then the equilibrium shape of the fully melted body (analysed by means of a general variational principle proved in §5); and finally the dynamics of the interior flow, which, as argued in §2, is likely to be turbulent when the levitated mass is of the order of a few grams or greater.

---

## 1. Introduction

If a piece of metal is placed in an alternating magnetic field, electric currents will be induced, interacting with the magnetic field to produce a Lorentz force which can support the metal against gravity. At the same time, the ohmic heating due to the induced currents can cause melting and result in a blob of liquid metal levitated by the applied field. This process, first suggested by Muck (1923) and reviewed† by Peifer (1965), has several advantages over the usual method of crucible melting: most obvious among these is that the liquid metal does not come into contact with a crucible wall so there is no danger of contamination, particularly by carbon and sulphur (in many metallurgical experiments see, for example, El-Kaddah & Robertson 1978 it is important to prepare very pure specimens as even small traces of impurities can affect the physical

† An excellent, although somewhat inaccessible, review of the literature up to 1975 is provided by Stephan (1975).

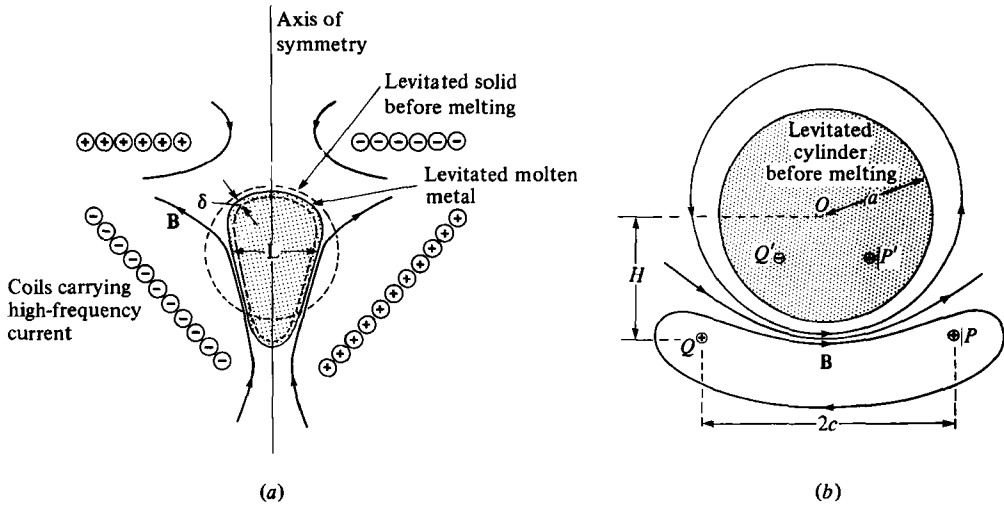


FIGURE 1. (a) Typical axisymmetric levitation device (after Okress *et al.* 1952); (b) idealised two-dimensional levitation device with parallel wires at  $P$  and  $Q$  carrying equal currents  $I \cos \omega t$ , and image currents  $-I \cos \omega t$  at the image points  $P'$ ,  $Q'$ .

properties); also the stirring of the liquid metal by the Lorentz force is an efficient method of mixing different metals in the production of alloys.

Levitation melting has been achieved by many experimenters, for example, Okress *et al.* (1952). A typical levitation device is sketched in figure 1a; the lower coil provides the main levitation force and the upper coil helps stabilise the metal against horizontal displacements. The frequency of the alternating current passed through the coils is typically of order  $10^4$  to  $10^5$  Hz and at such high frequencies the metal behaves as a perfect conductor, confining the field penetration to a thin surface layer; the metal is in effect supported by the magnetic pressure distribution over its surface.

Such levitation devices suffer from a number of problems. Firstly, in the configuration of figure 1a, the (approximately tangential) magnetic field on the metal surface vanishes at the highest and lowest points. At the lowest point the metal will tend to leak through the 'magnetic hole', and in some experiments the lower end becomes elongated and drips.† This is generally the crucial factor in limiting the mass of liquid metal that can be levitated. The levitated metal is also subject to a number of instabilities, and may rotate or vibrate rapidly. In spite of these difficulties, levitation melting has been successful for masses of order 100 g or more of various metals, and several commercial devices are available.

Some metallurgical processes also involve what might be called partial magnetic levitation – parts of the surface of a body of liquid metal being supported by magnetic field and others resting on solid supports. For example in the continuous casting of aluminium, the vertical walls of a column of the liquid metal are supported magnetically, while the base of the column rests on a solid ingot which is gradually moved downwards as more metal solidifies at the interface (Moreau 1980).

† This leakage is of course inhibited to some extent by surface tension. Moreover, various techniques have been tried, involving the use of two sets of coils carrying currents in time quadrature, for plugging the leak in a time-averaged manner (Zhezherin 1959).

Theoretical studies of levitation have so far dealt mainly with solid conductors.† Piggot & Nix (1966) have analyzed levitation of an infinitely long solid circular cylinder by a pair of equal and opposite alternating line currents, calculating stability boundaries and the rate of heating, and comparing theoretical and experimental results. It was found that (as is in fact generally true) the levitation force increases with the frequency, eventually tending to the perfectly conducting limit, and that the rate of heating increases indefinitely with frequency. Brisley & Thornton (1963) have carried out similar calculations for a solid sphere levitated by a number of coaxial circular coils. Harris & Stephan (1975) (see also Stephan 1975) have carried out a wide range of experiments on complete and partial levitation using sodium surrounded by a silicone oil, the metal having a low melting point and the buoyancy of the oil reducing the necessary levitation force. Some of these experiments illustrate a dramatic ‘folding’ instability of the metal surface, which has also been discussed by Zhezherin (1959). Volkov (1962) has analyzed the stability of a plane layer of liquid metal supported by a rapidly travelling magnetic field and has found that the fastest growing instabilities are those which extend along the magnetic field lines (i.e. the crests of the surface ripples running parallel to the magnetic field) but that these can be stabilised by sufficiently strong surface tension or magnetic field.

Magnetic levitation of liquid metals presents three interacting problems—the determination of the magnetic field, the unknown free surface shape, and the internal fluid motion. Most previous theoretical work—in particular the studies of solid levitation—has avoided the difficulty of the unknown free surface, and the closest approach to solving all three coupled problems seems to have been the paper by Volkov (1962), but even here only linearised departures from a simple equilibrium are involved. In the present paper we make some attempts at solving the coupled problems but only in situations where one of the three effects can be neglected. For example, we may study the coupling between the free surface shape and the magnetic field under the assumption that internal fluid motion can be neglected, or we may calculate the internal fluid motion under the assumption that the free surface shape is predetermined by strong surface tension. We consider in detail only two-dimensional problems, and in particular, levitation of an infinitely long cylinder by two parallel line currents in phase (figure 1*b*). This geometry‡ (which can be thought of as approximating a torus of large major radius) eliminates the difficulty due to the neutral magnetic field point which must occur at the bottom of a simply connected liquid-metal body in an axisymmetric configuration, and also enables us to use conformal transformation. We assume throughout that the alternating frequency is large, so that the magnetic field in the conductor is confined to a thin surface layer. The field lines outside the conductor are as sketched in the figure.

Section 2 uses the approximate formulae of Sneyd (1979) to show that the effect of the Lorentz force can be thought of as a magnetic pressure (which provides the levitation force) and a surface source of vorticity (which will generate internal fluid motion). Estimates of the strength of the internal flow are also given and it is concluded that this flow is likely to be turbulent in situations of interest. As a prelude to the study of fluid

† A parallel study to that reported here has been carried out by Mestel (1982) and cross-reference to this study will be made at appropriate points in the text.

‡ The suggestion that a cylindrical configuration may be advantageous is not new; it has been exploited in the so-called ‘boat crucible’ which levitates a cylinder of finite length (Peifer 1965).

levitation, §3 examines the levitation of a solid circular cylinder by parallel line currents in phase, calculating stability boundaries, and §4 examines the surface flow that develops during the initial stages of melting. Section 5 develops the general theory of fluid levitation when internal flow can be neglected, and it is shown that equilibrium can be determined by means of a variational principle involving gravitation, surface tension and magnetic energies. This principle is used to determine the shape for the special case of the cylindrical geometry. Finally, in §6, the dynamics of the turbulent flow within the levitated sample is considered; a uniform eddy viscosity is assumed, and a simple low Reynolds number analysis is used to give a first indication of the structure of the mean flow.

## 2. Order-of-magnitude considerations

A number of metals that have been melted in the levitated state (Peifer 1965) are listed in table 1*a*, together with some relevant physical properties (Smithells 1967). The masses levitated in useful contexts are generally in the range 1–100 g, and the typical span  $L$  of the levitated drop is generally in the range 5–30 mm.

We suppose that currents in the external coils produce a magnetic field

$$\mathbf{B} = \text{Re}(\mathbf{B}(\mathbf{x}) e^{i\omega t}). \quad (2.1)$$

For large  $\omega$ , this penetrates a small distance  $O(\delta)$  into the drop where

$$\delta = (2\omega\mu_0\sigma)^{-\frac{1}{2}}, \quad (2.2)$$

where  $\sigma$  is the electrical conductivity of the drop, and  $\mu_0 = 4\pi \times 10^{-7}$  (SI units). We suppose that

$$\delta \ll L. \quad (2.3)$$

Table 1*b* includes values of  $\delta$  for  $\omega/2\pi = 10^5$  Hz, and it will be clear that (2.3) is normally satisfied at frequencies of this order of magnitude.

Under condition (2.3), the field  $\mathbf{B}(\mathbf{x})$  in (2.1) is determined by the equations

$$\nabla \wedge \mathbf{B} = \mu_0 \mathbf{J}(\mathbf{x}), \quad \nabla \cdot \mathbf{B} = 0, \quad (2.4)$$

where  $\text{Re}(\mathbf{J}(\mathbf{x}) e^{i\omega t})$  represents the current that is concentrated in the external coils; the boundary conditions (to leading order in  $\delta/L$ ) are

$$\mathbf{B} \cdot \mathbf{n} = 0 \quad \text{on } S, \quad \mathbf{B} = O(r^{-3}) \quad \text{at } \infty, \quad (2.5)$$

where  $S$  is the surface of the drop.  $\mathbf{B}$  is clearly uniquely determined. If  $\mathbf{B} = \mathbf{B}_S$  on  $S$  (where  $\mathbf{B}_S$  is a tangential field) the mean magnetic pressure on  $S$  is

$$p_M = (4\mu_0)^{-1} \mathbf{B}_S \cdot \mathbf{B}_S^*, \quad (2.6)$$

and, as indicated in §1, it is essentially this pressure field which must support the sample. In order of magnitude, we must have

$$p_M L^2 \sim mg, \quad (2.7)$$

where  $m \sim L^3 \rho$  is the mass of the sample; equivalently, if  $B_0$  is a typical magnitude of  $|\mathbf{B}_S|$ , then, from (2.6) and (2.7)

$$B_0 / (\mu_0 \rho)^{\frac{1}{2}} \sim (gL)^{\frac{1}{2}}, \quad (2.8)$$

Metal	$T_m$ °C	$10^{-3}\rho$ kg/m <sup>3</sup>	$10^8\sigma$ Ω <sup>-1</sup> m <sup>-1</sup>	$\lambda$ m <sup>2</sup> /s	$10^5\kappa$ m <sup>2</sup> /s	$10^6\nu$ m <sup>2</sup> /s	$10^{-2}c_s$ J/kg/°C	$10^{-5}L_f$ J/kg	$\gamma$ N/m
Al	660	2.37	5.00	0.159	3.58	1.9	10.84	3.88	0.915
Cu	1083	8.24	4.74	0.168	3.23	0.55	4.94	2.04	0.135
Ga	29.8	6.10	3.87	0.206	1.35	0.33	4.08	0.80	0.735
In	157	7.03	3.02	0.264	2.17	0.24	2.74	0.28	0.559
Li	180	0.508	4.17	0.190	2.14	1.9	42.3	4.16	0.398
Pb	327	10.6	1.05	0.758	1.01	0.25	1.52	0.23	0.480

TABLE 1a. Physical properties of some liquid metals at (or just above) the melting point  $T_m$  (from Smithells 1967, converted to SI units);  $\rho$  = density,  $\sigma$  = conductivity,  $\lambda = (\mu_0\sigma)^{-1}$ ,  $\kappa$  = thermal diffusivity,  $\nu$  = kinematic viscosity,  $c_s$  = specific heat,  $L_f$  = latent heat of fusion,  $\gamma$  = surface tension.

Metal	$\delta$ = $(\lambda/2\omega)^{1/2}$ mm	$B_0$ = $(\mu_0\rho gL)^{1/2}$ T	$q_J$ = $\rho gL\lambda \delta$ J/m <sup>2</sup> /s	$\hat{v}$ = $q_J/\rho L_f$ mm/s	$t_m$ = $\rho Lc_s T_m/q_J$ s	$t_k$ = $L^3/\kappa$ s	$t_{\text{melt}}$ = $L/\hat{v}$ s	$h_{mc}$ = $(L^3\lambda\nu/\delta L_f)^{1/2}$ mm	$\epsilon$ = $L^2\rho g/\gamma$
Al	0.5	0.02	$7.5 \times 10^4$	0.08	230	2.8	125	$1.98 \times 10^{-2}$	2.6
Cu	0.5	0.03	$2.7 \times 10^5$	0.16	170	3.1	62.5	$4.5 \times 10^{-2}$	61
Ga	0.6	0.03	$2.2 \times 10^5$	0.45	3.4	7.4	22	$5.2 \times 10^{-2}$	8.3
In	0.7	0.03	$2.9 \times 10^5$	1.5	11	4.6	6.6	$6.9 \times 10^{-2}$	13
Li	0.6	0.008	$1.8 \times 10^4$	0.08	14	4.7	125	$5.2 \times 10^{-2}$	1.3
Pb	1.1	0.04	$7.3 \times 10^5$	3.0	7	9.9	3.3	$9.1 \times 10^{-2}$	22

TABLE 1b. Deduced orders of magnitude for levitation of the liquid metals of table 1a, with  $\omega = 2\pi \times 10^5$  Hz,  $L = 10$  mm.

i.e. the Alfvén velocity must be of the same order as the ‘free-fall’ velocity  $(gL)^{1/2}$  if levitation is to occur.

Let us now suppose that the flow inside the drop is characterised by a typical velocity  $u_0$ . We may then expect dynamic pressure variations of order  $\rho u_0^2$ , and an upper limit on  $u_0$  is given by the condition

$$\rho u_0^2 \lesssim p_M \sim \rho Lg, \tag{2.9}$$

since otherwise centrifugal forces would lead to fragmentation of the drop. The magnetic Reynolds number  $R_M = \mu_0 \sigma u_0 L$  then satisfies

$$R_M \lesssim \mu_0 \sigma (Lg)^{1/2} L, \tag{2.10}$$

i.e.  $R_M \lesssim 0.1$  for the fluids of table 1 with  $L \lesssim 30$  mm. This means that the field  $\mathbf{B}$  and current  $\mathbf{j}$  in the fluid volume  $V$  may be calculated neglecting the fluid motion, i.e. as if the sample were solid.

The Lorentz force in the surface layer has a mean part

$$\bar{\mathbf{F}} = \frac{1}{2} \text{Re}(\mathbf{j}^* \wedge \mathbf{B}), \tag{2.11}$$

and an oscillating part of frequency  $2\omega$ . The latter has a negligible effect when  $\omega$  is large, the response being limited by fluid inertia (aided by viscosity). We can therefore focus attention on the mean part (2.11). Boundary-layer methods (Sneyd 1979, particularly equations (2.17), (2.19)) show that, to leading order in  $\delta/L$ ,

$$\bar{\mathbf{F}} = 2\delta^{-1} p_M e^{-2w/\delta} \mathbf{n}, \tag{2.12}$$

$$\nabla \wedge \bar{\mathbf{F}} = -2\delta^{-1} (\mathbf{n} \wedge \nabla p_M) e^{-2w/\delta}, \tag{2.13}$$

where  $w$  is the distance from  $S$  in the direction of the inward normal  $\mathbf{n}$ . Integrating (2.12) and (2.13) across the magnetic boundary layer shows that the net effect of the Lorentz force is to provide (i) a surface pressure distribution  $p_M$  (as expected) and (ii) a surface source of vorticity  $-\mathbf{n} \wedge \nabla p_M$ . The surface pressure controls the shape of the sample and provides the levitating force, while the surface source of vorticity generates a rotational flow within the sample.

Let us first obtain some orders of magnitude that would follow from an assumption that the velocity field  $\mathbf{u}(\mathbf{x})$  is laminar and steady; it is purely meridional in the axisymmetric configuration of figure 1*a*, and two-dimensional in the configuration of figure 1*b*; in either case the streamlines are closed. The Navier–Stokes equations may be written in the form

$$\boldsymbol{\omega} \wedge \mathbf{u} + \nabla(\frac{1}{2}\mathbf{u}^2 + p/\rho + \mathbf{g} \cdot \mathbf{x}) = \rho^{-1}\bar{\mathbf{F}} - \nu\nabla\wedge\boldsymbol{\omega}, \quad (2.14)$$

where  $\boldsymbol{\omega} = \nabla \wedge \mathbf{u}$ , and integration round any closed streamline  $C$  gives

$$\rho\nu \oint_C \nabla \wedge \boldsymbol{\omega} \cdot d\mathbf{x} = \int_A \nabla \wedge \bar{\mathbf{F}} \cdot d\mathbf{S}, \quad (2.15)$$

where  $A$  is a surface spanning  $C$ . This equation provides an estimate for  $u_0$ ; for suppose that  $C$  passes partly through the magnetic boundary layer and partly through the fluid ‘core’, and let  $\omega_0 \sim u_0/L$  be a typical value of  $|\boldsymbol{\omega}|$ ; then within the surface layer†

$$|\nabla \wedge \boldsymbol{\omega}| \sim \omega_0/\delta, \quad (2.16)$$

(whereas in the core region,  $|\nabla \wedge \boldsymbol{\omega}| \sim \omega_0/L$ ), and (2.15) provides the estimate

$$\rho\nu(\omega_0/\delta)L \sim (\mu_0\delta)^{-1}(B_0^2/L)\delta L,$$

or equivalently

$$u_0 \sim \omega_0 L \sim B_0^2\delta/\rho\nu\mu_0 \sim gL\delta/\nu. \quad (2.17)$$

The corresponding Reynolds number is

$$R = u_0 L/\nu \sim gL^2\delta/\nu^2, \quad (2.18)$$

and this is generally very large for  $L \sim 10$  mm or greater. With  $\nu \sim 10^{-6}$  m<sup>2</sup>/s (see table 1) and with  $L \sim 10$  mm,  $\delta \sim 1$  mm, we find  $R \sim 10^6$ ! Flow at such large Reynolds numbers is of course likely to be unstable; the assumption of steady laminar flow therefore appears to be untenable.

Suppose then that the interior flow is turbulent, with both mean and fluctuating parts characterised by velocity scale  $u_0$  (which is of course no longer given by (2.17)). The force  $\bar{\mathbf{F}}$  will then be balanced primarily by the gradient of Reynolds stresses of order  $\rho u_0^2$ ; (2.15) is then replaced by

$$\oint_C \frac{\partial}{\partial x_j} (\rho u'_i u'_j) dx_i = \int_A \nabla \wedge \bar{\mathbf{F}} \cdot d\mathbf{S}, \quad (2.19)$$

† This estimate should be contrasted with the corresponding situation in a layer on a rigid surface, within which  $|\nabla \wedge \mathbf{u}| \sim u_0/\delta$ ,  $|\nabla \wedge \boldsymbol{\omega}| \sim u_0/\delta^2 \sim \omega_0 L/\delta^2$ . Mestel (1981) has arrived at the same estimate (2.17) through consideration of the rate of work of the force field  $\bar{\mathbf{F}}$ .

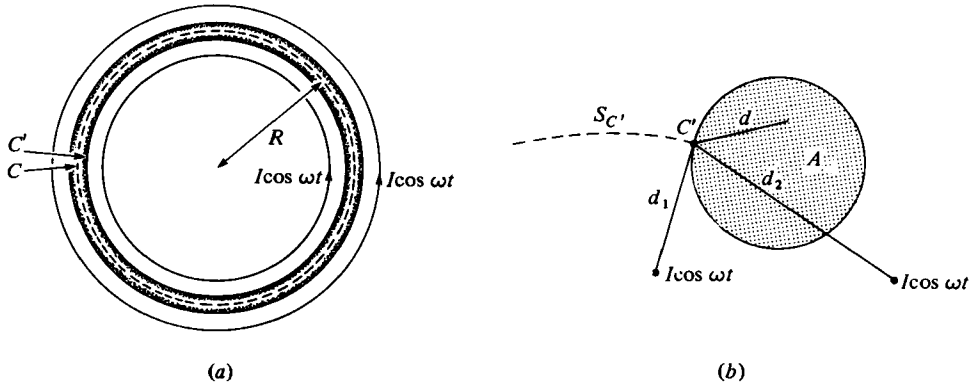


FIGURE 2. (a) Plan view, (b) cross-section, of levitated torus.

where  $\mathbf{u}'$  is the turbulent velocity; this gives an estimate  $\rho u_0^2 \sim B_0^2/\mu_0$ , or using (2.8),

$$u_0 \sim (gL)^{\frac{1}{2}}. \tag{2.20}$$

This estimate is much less than the estimate (2.17); it is moreover (just) consistent with the limit (2.9) set by the requirement that dynamic pressures be ‘contained’ by the magnetic pressure at the surface. It seems therefore that turbulence limits the level of internal velocity to the ‘free-fall’ scale, which is in any case maximal for ‘containment’ purposes. The associated Reynolds number is  $R \sim 3000$  (again using the data of Table 1).

As regards modelling the turbulence in this complicated context, it seems unlikely that one can do better (in the first instance) than assume a uniform eddy viscosity  $\nu_T \sim u_0 L$ , the associated Reynolds number  $R_T = u_0 L/\nu_T$  being then (by definition) of order unity. A low Reynolds number analysis of the mean flow should then give a qualitatively correct description, and this is the procedure we shall adopt later (see §6).

The possible presence of turbulence within the levitated drop is of great practical importance, as it will play a crucial role in mixing melt constituents and yielding a homogeneous product—one of the frequently quoted merits of the levitation-melting process (see, for example, Peifer 1965). Experimental evidence for the presence of turbulence is limited to observations of random ripples on the surface of levitated samples (Block & Theissen 1971; Stephan 1975); it seems likely that such ripples are simple surface perturbations associated with sub-surface turbulence, which cannot be directly detected.

### 3. Levitation of a solid circular cylinder by equal parallel currents in phase

We first consider the levitation and stability characteristics of the configuration of figure 1*b*, wherein the levitated body is a cylinder of circular cross-section (for the moment assumed solid). The solution to the external field problem (2.4), (2.5), is then easily solved by the method of images. With the notation of figure 1*b*, the image system for currents  $I \cos \omega t$  at  $P$  and  $Q$  are currents  $-I \cos \omega t$  at the image points  $P'$ ,  $Q'$ , and (possibly) a current  $I_1(t)$  at the centre of the cylinder. The total current flowing along the cylinder is then

$$I_{\text{tot}} = I_1 - 2I \cos \omega t.$$

For the case of a cylinder that is curved in the form of a torus  $\mathcal{T}$  with  $R \gg a$  (figure 2a),  $I_1$  is in fact zero for the following reason.† Consider the flux

$$\Phi = \int_{S_C} \mathbf{B} \cdot d\mathbf{S},$$

where  $S_C$  spans the curve  $C$  in figure 2a, passing along the axis of  $\mathcal{T}$ . Since  $\mathbf{B} \approx 0$  inside  $\mathcal{T}$ , we have equally

$$\Phi = \int_{S_{C'}} \mathbf{B} \cdot d\mathbf{S},$$

where  $C'$  is a circle on the surface of  $\mathcal{T}$ , as shown. Now

$$d\Phi/dt = -\oint_C \mathbf{E} \cdot d\mathbf{x} = 0,$$

since  $\mathbf{E} \approx 0$  in  $\mathcal{T}$ , and so  $\Phi = 0$  (all fields being periodic). Now, for large  $R$ , using a well-known formula for the mutual inductance of two circles,

$$\Phi \approx \mu_0 RI \cos \omega t \left( \ln \frac{R}{d_1} + \ln \frac{R}{d_2} \right) + \mu_0 R \int_A j \ln \left( \frac{R}{d} \right) dS,$$

where  $d_1, d_2, d$  are defined in figure 2b; hence, letting  $R \rightarrow \infty$ , with  $d_1, d_2, d$  fixed, we have

$$2I \cos \omega t + \int_A j dS = 2I \cos \omega t + I_{\text{tot}} = I_1 = 0, \quad (3.1)$$

as stated above.

#### Vertical equilibrium and stability

The lift force on the cylinder can be most simply calculated as the force on the image line currents, and has an average vertical component  $F_V$  given by

$$F_V = \frac{\mu_0 I^2}{2\pi} \left( \frac{\cos \alpha}{PP'} + \frac{\cos \beta}{PQ'} \right) = \frac{\mu_0 I^2}{2\pi c} G(\eta, k), \quad (3.2)$$

where (figure 1b)  $k = a/c$ ,  $\eta = H/c$  and the angles  $\alpha, \beta$  are as indicated in figure 4(a); hence

$$G(\eta, k) = \frac{\eta}{1 + \eta^2 - k^2} + \frac{\eta(1 + \eta^2 - k^2)}{(1 + \eta^2 - k^2)^2 + 4k^2}. \quad (3.3)$$

Figure 3 shows graphs of  $G(\eta, k)$  against  $\eta$  for various  $k$ . The behaviour of  $G$  depends on whether  $k < 1$  or  $k > 1$ , i.e. on whether the cylinder diameter is smaller or greater than the gap between the wires. When  $k < 1$ ,  $G$  attains a maximum, at  $\eta = \eta_1(k)$  say, and when  $k > 1$ ,  $G$  tends to infinity as  $\eta \rightarrow (k^2 - 1)^{1/2}$  at which point the cylinder is in contact with the wires.

Vertical equilibrium is given by  $F_V = mg$  where  $m$  is the cylinder mass/unit length, or from (3.2),

$$G(\eta, k) = 2\pi mgc / \mu_0 I^2 = W \quad \text{say}, \quad (3.4)$$

and the equilibrium is vertically stable provided

$$\partial G / \partial \eta < 0. \quad (3.5)$$

† For a straight cylinder of finite length,  $I_{\text{tot}} = 0$  and so  $I_1 = 2I \cos \omega t$ . The levitation force per unit length of cylinder is much less in this case than for the case of a torus.

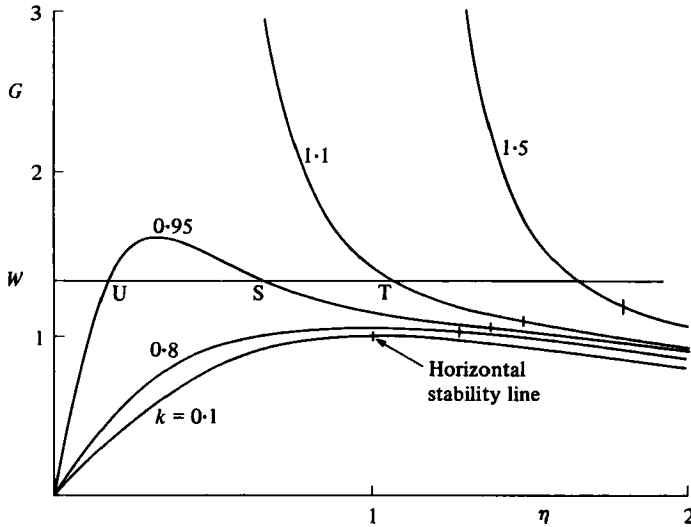


FIGURE 3. The function  $G(\eta, k)$ , given by equation (3.3), for various values of  $k$ . If  $k < 1$ , the equation  $G(\eta, k) = W$  can have two solutions; one of these ( $S$ ) represents a vertically stable equilibrium and one ( $U$ ) an unstable equilibrium. If  $k > 1$ , there is one stable equilibrium ( $T$ ). The vertical dashes represent the maximum value of  $\eta$  for horizontal stability.

For any given  $W$ , when  $k > 1$ , there is evidently a unique solution of (3.4) and this is stable; when  $k < 1$ , there are two solutions of (3.4) for  $\eta$ , but only the larger value satisfying

$$\eta > \eta_1(k), \tag{3.6}$$

represents a position of stable equilibrium.

### Horizontal stability

If the cylinder is displaced horizontally through a distance  $s$  (figure 4a), then the horizontal component of force on the cylinder due to the line current at  $P$  (which tends to restore equilibrium) is given by

$$F_H = \frac{\mu_0 I^2}{4\pi} \left( \frac{\sin \alpha}{PP'} + \frac{\sin \beta}{PQ'} \right). \tag{3.7}$$

The condition for horizontal stability is  $(dF_H/ds)_{s=0} > 0$ , or, from (3.7), after some calculation,

$$\eta < (1 + k^2)^{\frac{1}{2}} = \eta_2(k) \quad \text{say.} \tag{3.8}$$

When  $k < 1$ , stable equilibrium is possible only if

$$\eta_1(k) < \eta < \eta_2(k), \tag{3.9}$$

or equivalently if

$$W_1 > W > W_2, \tag{3.10}$$

where  $W_2 = G(\eta_2, k)$ . Table 2 lists  $\eta_1$ ,  $\eta_2$ ,  $W_1$  and  $W_2$  for  $0.05 \leq k \leq 0.95$ . The range  $W_1 - W_2$  of possible cylinder weights is extremely narrow for  $k \lesssim 0.8$ , but widens rapidly for larger  $k$ . On the curves of figure 3, the point  $\eta_2$  is marked by a vertical dash.

$k$	$W_1$	$W_2$	$\eta_1$	$\eta_2$
0.05	1.00000	1.00000	1.00121	1.00125
0.1	1.00001	1.00001	1.00489	1.00499
0.15	1.00006	1.00006	1.01093	1.01119
0.2	1.00019	1.00019	1.01901	1.0198
0.25	1.00046	1.00046	1.02889	1.03078
0.3	1.00094	1.00093	1.04027	1.04403
0.35	1.00169	1.00167	1.05268	1.05948
0.4	1.00282	1.00276	1.0657	1.07703
0.45	1.00441	1.00425	1.07877	1.09659
0.5	1.00657	1.00623	1.09135	1.11803
0.55	1.00943	1.00874	1.10267	1.14127
0.6	1.01317	1.01184	1.11168	1.16619
0.65	1.01801	1.01557	1.11684	1.19269
0.7	1.02432	1.01994	1.11552	1.22066
0.75	1.03274	1.025	1.10217	1.25
0.8	1.04479	1.03075	1.06043	1.28063
0.85	1.06865	1.03719	0.814221	1.31244
0.9	1.20086	1.04433	0.484192	1.34536
0.95	1.61832	1.05216	0.319122	1.37931

TABLE 2. Stability bounds for a levitated cylinder, as a function of the geometrical parameter  $k$ .

If  $k \gg 1$ , the sample will clearly become unstable when it melts (see §5 below and, particularly, figure 8); only values of  $k$  of order unity are therefore of practical interest, and for this reason we have restricted attention to the range  $0.5 \leq k \leq 1.5$  in subsequent computations.

#### Magnetic pressure distribution

It is a straightforward matter to calculate  $B_s$  and hence  $p_M$  on the cylinder surface. In the notation of figure 4*b*, we find

$$p_M = \frac{\mu_0 I^2}{16\pi^2 a^2} (l^2 - a^2)^2 \left( \frac{1}{r_1^2} + \frac{1}{r_2^2} \right)^2 = p_{M0} f(\theta), \quad (3.11)$$

where

$$p_{M0} = \mu_0 (I/4\pi a)^2 = \rho g c / 8\pi W, \quad (3.12)$$

and

$$f(\theta) = (1 - K^2)^2 \left[ \frac{1}{1 + K^2 - 2K \cos(\theta - \alpha)} + \frac{1}{1 + K^2 - 2K \cos(\theta + \alpha)} \right]^2, \quad (3.13)$$

with  $K = k(1 + \eta^2)^{-\frac{1}{2}}$ ,  $\alpha = \cot^{-1} \eta$ . The corresponding expression for  $-\mathbf{n} \wedge \nabla p_M$  (which appears in (2.3)) is

$$-\mathbf{n} \wedge \nabla p_M = a^{-1} p_{M0} f'(\theta) \hat{\mathbf{z}}, \quad (3.14)$$

where  $\hat{\mathbf{z}}$  is a unit vector along the cylinder axis. The function  $f(\theta)$  which plays an important part in the subsequent theory, is shown in figure 5 for various values of the geometrical parameters  $k$  and  $\eta$ .

#### The case $k = \eta = 1$

This case will be useful by way of example. With  $k = \eta = 1$ , we have  $K = 2^{-\frac{1}{2}}$  and  $\alpha = \frac{1}{4}\pi$ . From (3.3) and (3.4), this is a possible equilibrium if  $W = G(1, 1) = \frac{6}{5}$ , and it is stable. The function  $f(\theta)$  given by (3.12) simplifies in this case to

$$f(\theta) = 4 \left[ \frac{3 - 2 \cos \theta}{8 \cos^2 \theta - 12 \cos \theta + 5} \right]^2. \quad (3.15)$$

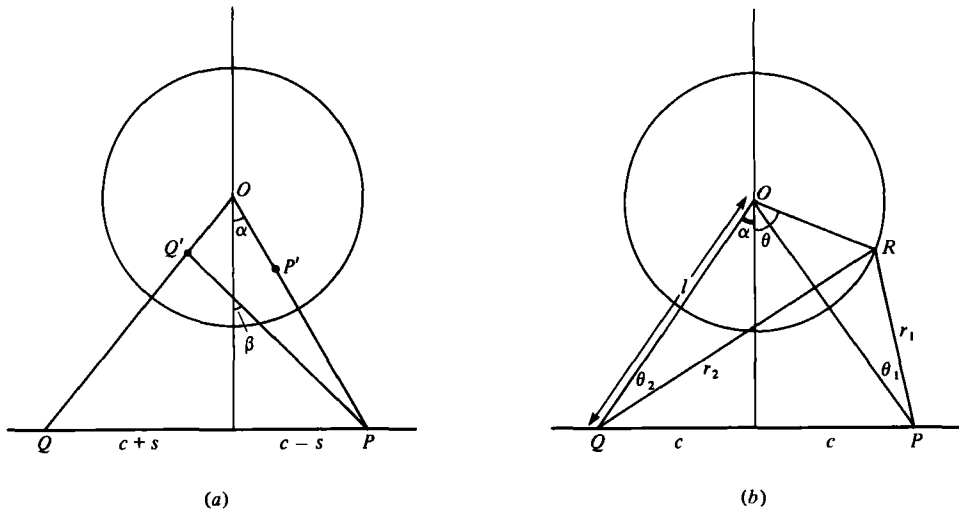


FIGURE 4. The levitated cylinder; (a) construction for determining horizontal stability; (b) notation for determination of  $p_M(\theta)$  on the cylinder surface, and the streamfunction  $\psi$  (§6).

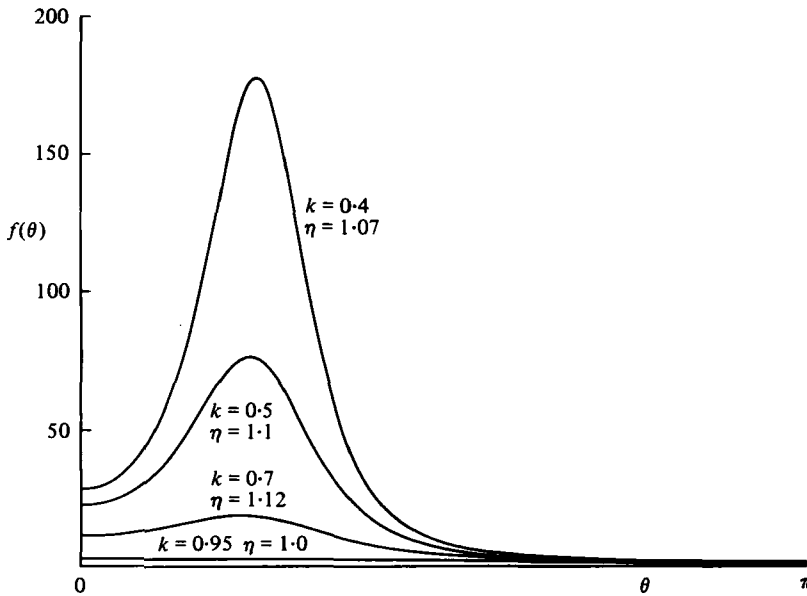


FIGURE 5. The function  $f(\theta)$  for various values of  $k$  and  $\eta$ .

#### 4. Flow in a surface film of molten metal

##### 4.1. General considerations

In this section, we study the initial stages of melting, the intermediate phase between solid and fluid levitation, when the solid is covered by a layer of molten metal so thin that viscous forces dominate and the methods of lubrication theory can be employed (see figure 6).

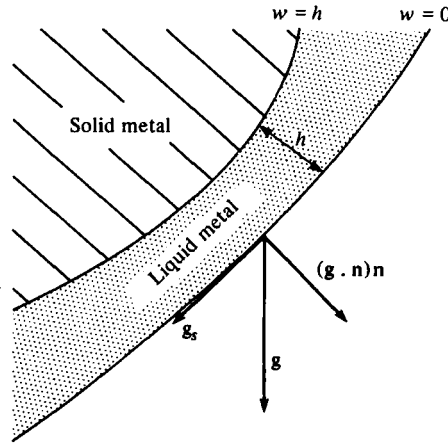


FIGURE 6. Notation for the thin film analysis of §4.

The mean rate of Joule heating per unit volume is

$$\overline{j^2}/\sigma = B_S^2 e^{-2w/\delta} / \mu_0^2 \delta^2 \sigma,$$

and so the mean rate of Joule heating per unit surface area (or equivalently the flux of electromagnetic energy through the surface) is

$$\int_0^\infty \overline{j^2}/\sigma dw = B_S^2 / 2\mu_0^2 \sigma \delta = q_J, \quad \text{say.} \quad (4.1)$$

In order of magnitude, using (2.8), we have

$$q_J \sim \rho g L \lambda / \delta. \quad (4.2)$$

Now the total heat supplied per unit time is  $\sim L^2 q_J$ , and, provided the variation in temperature throughout the sample is not too great, this is of order  $(\rho L^3) c_s \Delta T$ , where  $\Delta T$  is the increase in temperature in unit time and  $c_s$  is the specific heat of the metal; hence the time  $t_m$  to raise the temperature from  $0^\circ\text{C}$  to the melting point  $T_m$  is

$$t_m \sim \rho L c_s T_m / q_J. \quad (4.3)$$

This is compared with the diffusion time  $t_\kappa$  in table 1b; for the best conductors,  $t_m \gg t_\kappa$ , and for the others,  $t_m$  and  $t_\kappa$  are of the same order of magnitude. This means that thermal diffusion is generally strong enough to spread the heat fairly uniformly through the sample during the melting process. Once melting begins, the rate of advance of the liquid/solid interface is

$$\hat{v} \sim q_J / \rho L_f, \quad (4.4)$$

where  $L_f$  is the latent heat of fusion, and the time to complete the melting is

$$t_{\text{melt}} \sim L / \hat{v} \quad (4.5)$$

(see also table 1b).

Using the expression (2.12) for  $\overline{\mathbf{F}}$ , the normal component of the equation of motion in the layer (in the lubrication approximation) is

$$-\partial p / \partial w + (2p_M / \delta) e^{-2w/\delta} + \rho \mathbf{g} \cdot \mathbf{n} = 0. \quad (4.6)$$

Here, by virtue of (2.8), the gravitational term is smaller by a factor  $O(\delta/L)$  than the magnetic term and may be neglected. Since  $p = 0$  on  $w = 0$  (neglecting a surface tension contribution),

$$p = p_M(1 - e^{-2w/\delta}). \quad (4.7)$$

If the layer thickness  $h$  is small compared with  $\delta$ , then (4.7) gives

$$p \approx 2(w/\delta)p_M, \quad (4.8)$$

while, if  $h \gg \delta$ ,  $p \approx p_M$  throughout the fluid layer except in the magnetic skin.

Substitution of (4.7) in the tangential projection of the equation of motion gives (in the same lubrication approximation)

$$\rho\nu(\partial^2\mathbf{u}/\partial w^2) = (1 - e^{-2w/\delta})\nabla_S p_M - \rho\mathbf{g}_S, \quad (4.9)$$

where  $\mathbf{g}_S = \mathbf{g} - \mathbf{n}(\mathbf{g} \cdot \mathbf{n})$ ,  $\nabla_S = \nabla - \mathbf{n}(\mathbf{n} \cdot \nabla)$ . The solution of (4.9) satisfying  $u = 0$  on  $w = h$  and  $\partial\mathbf{u}/\partial w = 0$  on  $w = 0$  is

$$\mathbf{u} = \frac{1}{2\nu}(h^2 - w^2)\mathbf{g}_S + \frac{1}{4\rho\nu}[2(h-w)(\delta - w - h) - \delta^2(e^{-2w/\delta} - e^{-2h/\delta})]\nabla_S p_M, \quad (4.10)$$

and the corresponding flux  $\mathbf{Q}$  in the layer is

$$\mathbf{Q} = \int_0^h \mathbf{u} dw = \frac{h^3}{3\nu}\left(\mathbf{g}_S - \rho^{-1}F\left(\frac{h}{\delta}\right)\nabla_S p_M\right), \quad (4.11)$$

where

$$F(x) = 1 - \frac{3}{8x^3}(2x^2 - 1 + (2x + 1)e^{-2x}). \quad (4.12)$$

The two limiting cases mentioned above correspond here to the limiting behaviour

$$F \sim \begin{cases} \frac{3}{4}x & (x \ll 1), \\ 1 & (x \gg 1). \end{cases} \quad (4.13)$$

Allowing now for the advance of the liquid/solid interface due to melting, the fluid conservation equation takes the form

$$\frac{\partial h}{\partial t} + \nabla \cdot \mathbf{Q} = \frac{q_J}{\rho L_f} = \frac{2\lambda}{\rho L_f \delta} p_M. \quad (4.14)$$

It is clear that, when  $h$  is sufficiently small, the melting term in (4.14) dominates, and  $h$  grows in proportion to  $p_M$ . When  $h = O(h_{mc})$ , where

$$h_{mc} = (L^2\lambda\nu/L_f\delta)^{\frac{1}{2}}, \quad (4.15)$$

the melting and convection terms in (4.14) are of the same order of magnitude; and when  $h \gg h_{mc}$ , the convection term  $\nabla \cdot \mathbf{Q}$  dominates;  $h_{mc}$  is generally in the range 0.01–0.1 mm (see table 1b).

There is of course also an upper limit on  $h$  for the validity of the lubrication approximation. From (4.11), the flux within the layer is of order  $h^3g/\nu$ , and the Reynolds number is then  $\sim h^3g/\nu^2$ . The lubrication approximation requires that  $(h^3g/\nu^2)(h/L) \lesssim 1$ , i.e.

$$h \lesssim (L\nu^2/g)^{\frac{1}{2}} = h_1 \text{ say.} \quad (4.16)$$

For the typical liquid metals of table 1, this gives the astonishingly low estimate  $h_l \sim 0.1$  mm! It is hard to believe that inertial effects could become important for  $h \lesssim 1$  mm, and yet this does seem to be an inevitable consequence of the very small kinematic viscosity of liquid metals.

It follows from these orders of magnitude that, for so long as lubrication theory is valid, the approximation  $h \ll \delta$  is also likely to be satisfied, and then (4.11) becomes

$$Q \sim \frac{h^3}{3\nu} \left( \mathbf{g}_S - \frac{3}{4}\rho^{-1} \frac{h}{\delta} \nabla p_M \right). \quad (4.17)$$

Here, the magnetic effect is *small* compared with the gravitational effect, and the layer simply drains under gravity as soon as it is formed, the levitating force being located predominantly within the solid metal.

This conclusion is rather uninteresting from a fluid dynamical point of view. A more interesting behaviour can however arise if the field frequency is increased to the point at which  $\delta \ll h$ , when (4.11) becomes

$$Q \sim \frac{h^3}{3\nu} (\mathbf{g}_S - \rho^{-1} \nabla p_M). \quad (4.18)$$

Now the magnetic pressure term competes with gravity on an equal basis in determining the film evolution.

#### 4.2. Surface layer in the levitated cylinder

This behaviour is well illustrated by the case of the levitated cylinder, for which  $p_M$  is given by (3.14) and (3.15). Hence from (4.11), the flux  $Q(\theta)$  in the layer is given by

$$Q \sim -\frac{h^3 g}{3\nu} \left( \sin \theta + \frac{F(h/\delta)}{8Wk} f'(\theta) \right), \quad (h \gg \delta), \quad (4.19)$$

and (4.14) becomes

$$\frac{\partial h}{\partial t} + \frac{1}{a} \frac{\partial Q}{\partial \theta} = \frac{2\lambda p_{M0}}{\rho L_f \delta} f(\theta), \quad (4.20)$$

from which the evolution of the film may be computed.

For the particular case  $k = \eta = 1$ , (and  $W = \frac{6}{5}$ ), using (3.13), (4.15) becomes (with  $\mu = \cos \theta$ )

$$Q = -\frac{h^3 g}{3\nu} \sin \theta \left[ 1 - \frac{5}{3} \frac{F(h/\delta) (3 - 2\mu) (8\mu^2 - 12\mu + 13)}{(8\mu^2 - 12\mu + 5)^3} \right]. \quad (4.21)$$

When  $h \gg \delta$ , so that  $F(h/\delta) \sim 1$ , this flux is positive for  $\mu > 0.108$  (i.e. for  $|\theta| < 83.8^\circ$ ), and it is negative for  $|\theta| > 83.8^\circ$ . The fluid in the layer is then driven by the combination of magnetic pressure and gravity towards the points  $\theta = \pm 83.8^\circ$ . Obviously the layer thickness builds up according to (4.20) in a neighbourhood of these points until lubrication theory ceases to be valid.

## 5. Magnetostatic analysis

### 5.1. General considerations

In this section, we shall obtain some exact results concerning the shape of a levitated drop, under the assumption that effects associated with the interior motion may be neglected; the shape is then determined by a static balance between gravitational, surface tension and magnetic forces.

In the fluid core, where  $\bar{\mathbf{F}} = 0$ , the pressure is hydrostatic, i.e.

$$p = p_0 - \rho g x, \quad (5.1)$$

where  $x$  is vertically upwards and  $p_0$  is constant. In the magnetic boundary layer (cf (4.7)),

$$p = p_M(1 - e^{-2w/\delta}) + \gamma\kappa, \quad (5.2)$$

where we now include the effect of surface tension  $\gamma$ ;  $\kappa$  is the sum of the principal surface curvatures. Since (5.2) tends to (5.1) as  $w/\delta \rightarrow \infty$ , we obtain the natural boundary condition on  $S$ ,†

$$\gamma\kappa + p_M + \rho g x = \text{cst. on } S. \quad (5.3)$$

We now aim to convert (5.3) into a variational principle, which will be useful for the computation of stable equilibria. This principle involves the energies

$$U_g = \int_V \rho g x d\tau, \quad U_\gamma = \gamma A_S, \quad U_M = \int_{\hat{V}} \frac{1}{4\mu_0} |\mathbf{B}|^2 d\tau, \quad (5.4)$$

associated with the gravity, surface tension and magnetic field.‡ where  $A_S$  is the area of  $S$ , and  $\hat{V}$  is the exterior domain. Suppose that the surface  $S$  is perturbed by a small amount  $\delta h \mathbf{n}$  subject to the constraint that the volume of liquid remains constant, i.e.

$$\delta \int_V d\tau = \int_S \delta h dS = 0, \quad (5.5)$$

and subject also to the condition that the currents in the external coils remain at constant amplitude. Then the associated changes in  $U_g$  and  $U_\gamma$  are

$$\left. \begin{aligned} \delta U_g &= \int_S \rho g x \delta h dS, \\ \delta U_\gamma &= \gamma \delta A_S = \gamma \int_S \kappa \delta h dS, \end{aligned} \right\} \quad (5.6)$$

and the change in  $U_M$  is

$$\delta U_M = - \int_S \frac{1}{4\mu_0} |\mathbf{B}|^2 \delta h dS + \text{Re} \int_{\hat{V}} \frac{1}{2\mu_0} \mathbf{B}^* \cdot \delta \mathbf{B} d\tau. \quad (5.7)$$

Now let  $\mathbf{B} = \mathbf{B}_1 + \mathbf{B}_2$ , where  $\mathbf{B}_1$  is the field due to the currents in the external coils in the absence of any levitated material (so that  $\delta \mathbf{B}_1 = 0$ ), and  $\mathbf{B}_2$  is the field due to the induced currents in  $V$ , so that  $\nabla \wedge \mathbf{B}_2 = 0$ , i.e.  $\mathbf{B}_2 = \nabla \phi_2$  say, in  $\hat{V}$ . Then

$$\begin{aligned} \int_{\hat{V}} \mathbf{B}^* \cdot \delta \mathbf{B} d\tau &= \int_{\hat{V}} \mathbf{B}^* \cdot \nabla \phi_2 d\tau = \int_{\hat{V}} \nabla \cdot (\mathbf{B}^* \phi_2) d\tau \\ &= \int_S (\mathbf{n} \cdot \mathbf{B}^*) \phi_2 dS = 0, \end{aligned}$$

† With  $B = \nabla \phi$  and  $p_M = (4\mu_0)^{-1}(\nabla \phi)^2$ , (5.3) is identical with the dynamic boundary condition at the free surface of a steady incompressible irrotational inviscid flow with velocity potential  $\phi$ , provided  $(4\mu_0)^{-1}$  is identified with  $(2\rho)^{-1}$ . In both cases,  $\phi$  is a harmonic function satisfying  $\partial \phi / \partial n = 0$  on  $S$ ; but when  $\phi$  represents a velocity potential, its domain is the interior of  $S$ , whereas in the magnetic case its domain is the exterior.

‡ To get a finite value for  $U_M$ , the distribution of current in the external coils must be regarded as continuous, so that the sources for  $\mathbf{B}$  are not singular. Alternatively, the singular part can be subtracted out, as done later in § 5.3.

and so (5.7) becomes

$$\delta U_M = - \int_S p_M \delta h dS. \quad (5.8)$$

It follows from (5.6) and (5.8) that

$$\delta(U_g + U_\gamma - U_M) = \int_S (\gamma\kappa + p_M + \rho gx) \delta h dS. \quad (5.9)$$

Hence the boundary condition (5.3), together with the constraint (5.5), implies that

$$\delta(U_g + U_\gamma - U_M) = 0, \quad (5.10)$$

and conversely, the variational statement (5.10), subject to (5.5), implies (5.3). Note the appearance of the minus sign in (5.10): the variation in the total energy ( $U_g + U_\gamma + U_M$ ) is not zero, but is equal to  $2\delta U_M$ , the work done in the external circuits to maintain currents of constant amplitude.

Note also that the principle (5.10) holds also for a *solid* levitated body, with  $U_\gamma = 0$ . It has been used in this form by some authors (e.g. Hatch 1965) to analyse positions of equilibria; but the above proof applied to general fluid equilibria appears to be new.†

### 5.2. The levitated fluid cylinder; strong surface tension

For the levitated cylinder problem, we may first obtain an analytic indication of the equilibrium shape, by supposing that surface tension is strong so that the cross-section is approximately circular. Specifically, let

$$mg/\gamma = \epsilon \ll 1, \quad (5.11)$$

and let the equation of the cylinder surface‡ be

$$r = a_0 \left[ 1 + \epsilon \sum_{n=2}^{\infty} a_n \cos n\theta + O(\epsilon^2) \right], \quad (5.12)$$

the  $n = 1$  term being omitted since this corresponds simply to a vertical displacement of the centre. The cross-sectional area is

$$\pi a^2 = \frac{1}{2} \int_0^{2\pi} r^2 d\theta = \pi a_0^2 \left( 1 + \frac{1}{2} \epsilon^2 \sum_{n=2}^{\infty} a_n^2 \right), \quad (5.13)$$

and so, in the linearized analysis that follows, we may take  $a_0 = a$ .

In equation (5.3), using (3.11) and (3.12),

$$\begin{aligned} p_M + \rho gx &= \rho g \left( x + \frac{c}{8W} f(\theta) \right) \\ &= \frac{\gamma\epsilon}{\pi a} \left( \cos \theta + \frac{1}{8kW} f(\theta) \right) + O(\epsilon^2), \end{aligned} \quad (5.14)$$

† A variational principle analogous to (5.10) has been established by Brancher & Sero Guillaume (1981) in the context of a *ferromagnetic* fluid subjected to a static magnetic field, and under the influence of gravity and surface tension.

‡ A fluid cylinder, levitated in the manner envisaged here, might be subject to longitudinal instabilities; these could presumably be stabilized by the application of a sufficiently strong longitudinal high frequency field, as in analogous plasma contexts; for present purposes we ignore them.

An approximation of the form (5.11), (5.12) has been adopted also by Mestel (1982) in an investigation of the effect of interior motion on free surface shape.

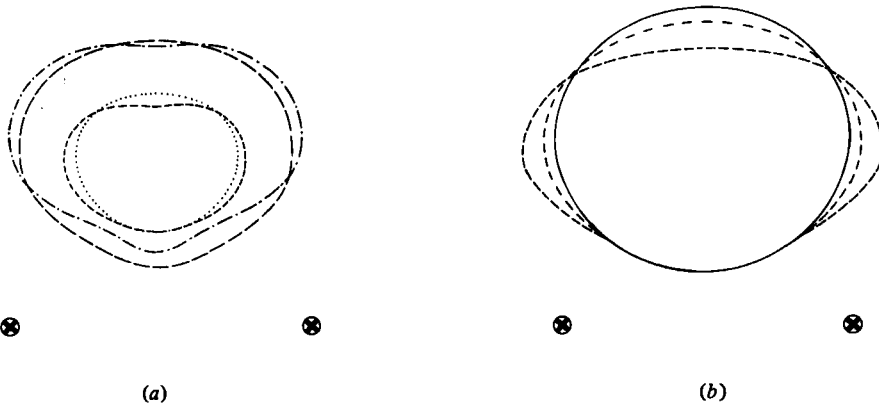


FIGURE 7. Cross-sectional shapes of levitated molten cylinder. (a) Calculated by perturbation procedure:  $\cdots$   $k = 0.5$ ,  $\eta = 1.1$ ,  $\epsilon = 16$ ;  $----$   $k = 0.5$ ,  $\eta = 1.1$ ,  $\epsilon = 32$ ;  $————$   $k = 0.8$ ,  $\eta = 1.2$ ,  $\epsilon = 15$ ;  $-----$   $k = 0.8$ ,  $\eta = 1.2$ ,  $\epsilon = 30$ . (b) Calculated numerically using variational principle: ( $k = 1$ )  $————$   $\Gamma = 1$ ,  $W = 1.07$ ;  $-----$   $\Gamma = 0.3$ ,  $W = 1.081$ ;  $————$   $\Gamma = 0.1$ ,  $W = 1.096$ .

and the curvature  $\kappa$  is given by

$$\begin{aligned} \kappa &= (r^2 + 2r'^2 - rr'') (r^2 + r'^2)^{-\frac{3}{2}} \\ &= a^{-1} \left( 1 + \epsilon \sum_{n=2}^{\infty} (n^2 - 1) a_n \cos n\theta + O(\epsilon^2) \right). \end{aligned} \quad (5.15)$$

Hence, to order  $\epsilon$ , (5.3) gives

$$\sum_{n=2}^{\infty} (n^2 - 1) a_n \cos n\theta + \frac{1}{\pi} \cos \theta + \frac{1}{8\pi k W} f(\theta) = \text{cst.} \quad (5.16)$$

If we now expand  $f(\theta)$  as a Fourier cosine series

$$f(\theta) = \frac{1}{2} f_0 + \sum_{n=1}^{\infty} f_n \cos n\theta, \quad (5.17)$$

then, from (5.18),

$$a_n = - \frac{f_n}{8\pi k W (n^2 - 1)}, \quad (n = 2, 3, \dots). \quad (5.18)$$

A numerical method was used to calculate the  $f_n$ , and hence to obtain the surface perturbation for various values of  $k$  and  $\eta$  ( $W$  being given by (3.3), (3.4)); figure 7a shows cross-sections calculated in this way. The effect of magnetic pressure in the regions closest to the line currents is quite evident.

### 5.3. The levitated fluid cylinder; weak surface tension

When surface tension is weak, the perturbation from circular shape will be large, and a numerical method must be adopted. We shall use the variational principle (5.10) to determine the shape. It is convenient also to adopt complex variable techniques.

The plane of cross-section of the fluid cylinder is taken to be the complex  $z$ -plane and for convenience the  $x$ -axis chosen as the axis of symmetry. Applying the Riemann Mapping Theorem to the exterior of  $S$  shows that there exists a unique analytic function

$\zeta(z)$  which transforms the free surface  $S$  to the unit circle  $|\zeta| = 1$  in such a way that  $\zeta(\infty) = \infty$ ,  $\zeta'(\infty)$  is real. The inverse function  $z(\zeta)$  is also analytic and can be expanded as a Laurent series

$$z = C_1 \zeta + c_0 + \sum_{n=1}^{\infty} c_n \zeta^{-n}. \quad (5.19)$$

By symmetry the  $c_n$  and  $C_1$  are all real.

Since the cross-sectional area inside  $S$  is fixed,

$$\frac{1}{2} \text{Im} \int_S \bar{z} dz = \pi a^2.$$

Substitution from (5.19) gives

$$\frac{1}{2} \text{Im} \int_{S'} \left( \frac{C_1}{\zeta} + c_0 + \sum_{n=1}^{\infty} c_n \zeta^n \right) \left( C_1 - \sum_{n=1}^{\infty} \frac{nc_n}{\zeta^{n+1}} \right) d\zeta = \pi a^2,$$

since  $\zeta \bar{\zeta} = 1$  on  $S'$ , and evaluation by Cauchy's Theorem gives

$$C_1^2 = a^2 + \sum_{n=1}^{\infty} nc_n^2. \quad (5.20)$$

Our strategy will be to choose the  $c_n$  as independent variables, and to express  $U = U_g + U_\gamma - U_M$  in terms of these variables; Numerical minimization will determine the  $c_n$ .

*Expression for  $U_g$ :*

$$U_g = \rho g \int_{A_c} x dx dy = \rho g \int_S \frac{1}{2} x^2 dy = \rho g \int_{|\zeta|=1} \frac{1}{2} x^2 \frac{dy}{d\zeta} d\zeta.$$

Substitution from (5.19) gives

$$U_g = \frac{1}{2} \rho g \int_0^{2\pi} \left( C_1 \cos \theta + \sum_{n=0}^{\infty} c_n \cos n\theta \right)^2 \left( C_1 \cos \theta - \sum_{n=1}^{\infty} nc_n \cos n\theta \right) d\theta,$$

and evaluating the various trigonometric integrals

$$\frac{U_g}{\rho g} = \pi C_1^2 c_0 - \pi c_0 \sum_{n=1}^{\infty} nc_n^2 - \pi C_1 \sum_{n=1}^{\infty} nc_n c_{n+1} - \frac{\pi}{4} \sum_{m=1}^{\infty} \sum_{n=1}^{\infty} (m+3n) c_m c_n c_{m+n}. \quad (5.21)$$

*Expression for  $U_\gamma$ :*

$$U_\gamma = \gamma l,$$

where  $l$  is the length of  $S$ . It will not be possible to write an algebraic formula for  $l$  in terms of the  $c_n$  – for example when  $c_n = 0$  for  $n \geq 2$  then  $S$  is an ellipse and the expression for the perimeter of an ellipse in terms of its major and minor axes involves elliptic integrals – so an approximate method must be used.

Let  $r(\zeta)$  be an analytic function with a Laurent expansion

$$r(\zeta) = r_0 + \sum_{n=1}^{\infty} r_n \zeta^{-n}, \quad (5.22)$$

such that

$$r^2(\zeta) = \frac{dz}{d\zeta} = C_1 - \sum_{n=1}^{\infty} \frac{nc_n}{\zeta^{n+1}}. \quad (5.23)$$

Substitution of (5.22) into (5.23) shows that the coefficients  $r_n$  can be determined by the recursive scheme  $r_0 = C_1^{\frac{1}{2}}$ ,  $r_1 = 0$ ,

$$r_n = -\frac{1}{2r_0} \left[ (n-1)c_{n-1} + \sum_{m=2}^{n-2} r_m r_{n-m} \right], \quad (n = 2, 3, \dots)$$

Then

$$l = \int_S |dz| = \int_{S'} |dz/d\zeta| |d\zeta| = \int_{S'} r(\zeta) \bar{r}(\zeta) d\theta,$$

so

$$U_\gamma = 2\pi\gamma \sum_{n=0}^{\infty} r_n^2. \tag{5.24}$$

*Expression for  $U_M$ :*

The field near each line current gives an infinite contribution to the magnetic energy, but these singularities can be removed by defining

$$U_M = \lim_{r \rightarrow 0} \left\{ \frac{1}{4\mu_0} \int_{\hat{A}_r} B^2 dx dy + \frac{\mu_0 I^2}{4\pi} \ln r \right\} \tag{5.25}$$

where  $\hat{A}_r$  is the exterior of the cylinder excluding two circles of radius  $r$  centred on the line currents at  $P$  and  $Q$ . If  $f(z)$  is the complex potential for  $\mathbf{B}$ , then

$$B = |df/dz|,$$

and the magnification of the conformal transformation from the  $z$ -plane to the  $\zeta$ -plane is  $|d\zeta/dz|$  so that if  $\zeta = \sigma + i\tau$

$$\frac{\partial(\sigma, \tau)}{\partial(x, y)} = \left| \frac{d\zeta}{dz} \right|^2.$$

Transformation of the integral in (5.25) gives

$$U_M = \lim_{r \rightarrow 0} \left\{ \int_{\hat{A}'_r} \left| \frac{df}{d\zeta} \right|^2 d\sigma d\tau + \frac{\mu_0 I^2}{4\pi} \ln r \right\}, \tag{5.26}$$

where  $\hat{A}'_r$  is the region of the  $\zeta$ -plane corresponding to  $\hat{A}_r$  and  $r'$  the radius of the corresponding small circles around the line currents. Now

$$\ln r = \ln r' + \ln(r/r') \rightarrow \ln r' + \ln |dz/d\zeta|_P \quad \text{as } r \rightarrow 0,$$

so (5.26) can be written in the form

$$U_M = \lim_{r \rightarrow 0} \left\{ \frac{1}{4\mu_0} \int_{\hat{A}'_r} \left| \frac{df}{d\zeta} \right|^2 d\sigma d\tau + \frac{\mu_0 I^2}{4\pi} \ln r' \right\} + \frac{\mu_0 I^2}{4\pi} \ln \left| \frac{dz}{d\zeta} \right|_P = U'_M + \frac{\mu_0 I^2}{4\pi} \ln \left| \frac{dz}{d\zeta} \right|_P, \tag{5.27}$$

where  $U'_M$  is the magnetic energy of the field in the  $\zeta$ -plane. This simple relation between  $U_M$  and  $U'_M$  is what makes a conformal transformation method so convenient.

To calculate  $U_M$  the point  $P'$  in the  $\zeta$ -plane, corresponding to  $P$ , was located by Newton iteration on the equation  $z_P = z(\zeta_{P'})$ ; then  $U'_M$  could be found by image methods.

### Minimization

The series (5.19) was truncated after  $N$  terms, so that  $U = U(c_0, c_1, \dots, c_N)$ . The series (5.22) was truncated after 15 terms, since retention of further terms had no effect on

$N$	$W_1$ : maximum $W$ for stable levitation	$W_2$ : minimum $W$ for stable levitation
3	1.043 25	1.036 39
5	1.042 89	1.036 01
7	1.042 84	1.036 00
9	1.042 84	1.036 00

TABLE 3. Convergence of results for increasing  $N$ ;  $k = 0.8$ ,  $\Gamma = 1.0$ .

the results. The function  $U$  was minimised using the NAG subroutine E04DFF, which is based on a modified-Newton algorithm, and the calculations carried out on the University of Waikato Vax 11/780 computer. The programme was checked by setting  $N = 0$ , which constrains the cylinder cross-section to be circular, and the results of table 2 were reproduced. Convergence was checked by running the programme for various  $N$ , and table 3 shows a typical set of results. For the bulk of the calculations,  $N$  was set equal to 4, in which case each minimization took approximately 3 seconds of c.p.u. time.

Horizontal stability could be tested in a simple way. Only  $U_M$  is affected by a rigid horizontal displacement of the fluid cylinder, which is represented mathematically by the addition of a purely imaginary constant to (5.19). Since  $dz/d\zeta$  is unaffected, the stability depends only on the first term of (5.27) so the criterion for horizontal stability is just (3.8) applied to the  $\zeta$ -plane cylinder.

The maximum  $W$  (dimensionless cylinder weight), for which levitation is possible, with fixed values of the other parameters, was determined by increasing  $W$  gradually until no minimum of  $U$  could be found.

### Results

The dimensionless parameters which can be independently varied are  $k = a/c$ , where the cross-sectional area is  $\pi a^2$ ,  $W = 2\pi cmg/\mu_0 I^2$ , and

$$\Gamma = \pi\gamma c/\mu_0 I^2 = W/\epsilon, \quad (5.28)$$

which provides a dimensionless measure of surface tension relative to magnetic forces. Figure 7*b* shows three cross-sections (for  $k = 1.0$ ) which show the effect of decreasing  $\Gamma$ . When  $\Gamma = 1$  the perturbation from the circular shape is still small, and as  $\Gamma$  decreases the change in shape is qualitatively similar to that predicted by the linear theory of §5.2.

For given  $k$  and  $\Gamma$ , there is a range of values of  $W$  over which stable levitation can occur, the width of this range increasing to a maximum as  $\Gamma$  tends to infinity (at which point the results are the same as for the rigid cylinder). Figure 8*a* shows stability boundaries in the range  $0 \leq \Gamma \leq 1$  for  $k = 0.7, 1.0$  and  $1.5$ . For  $k < 0.788$  stable levitation is possible with  $\Gamma = 0$ , but for  $k > 0.788$  it is possible only if  $\Gamma > \Gamma_m(k)$  (see Figure 8*b*). If  $\Gamma < \Gamma_m(k)$  the lateral spread becomes so great that the fluid in effect spills over the edges of the magnetic well;  $k$  then decreases to the value  $k_1$  at which  $\Gamma_m(k_1) \approx \Gamma$  and surface tension can then just retain the sample within the stability limit.

The lower stability limit for  $W$  is determined by the horizontal stability criterion referred to above. If  $W$  is decreased (by decreasing  $m$ , keeping other parameters fixed), the sample rises until criterion (3.8) (adapted to the  $\zeta$ -plane) is violated.

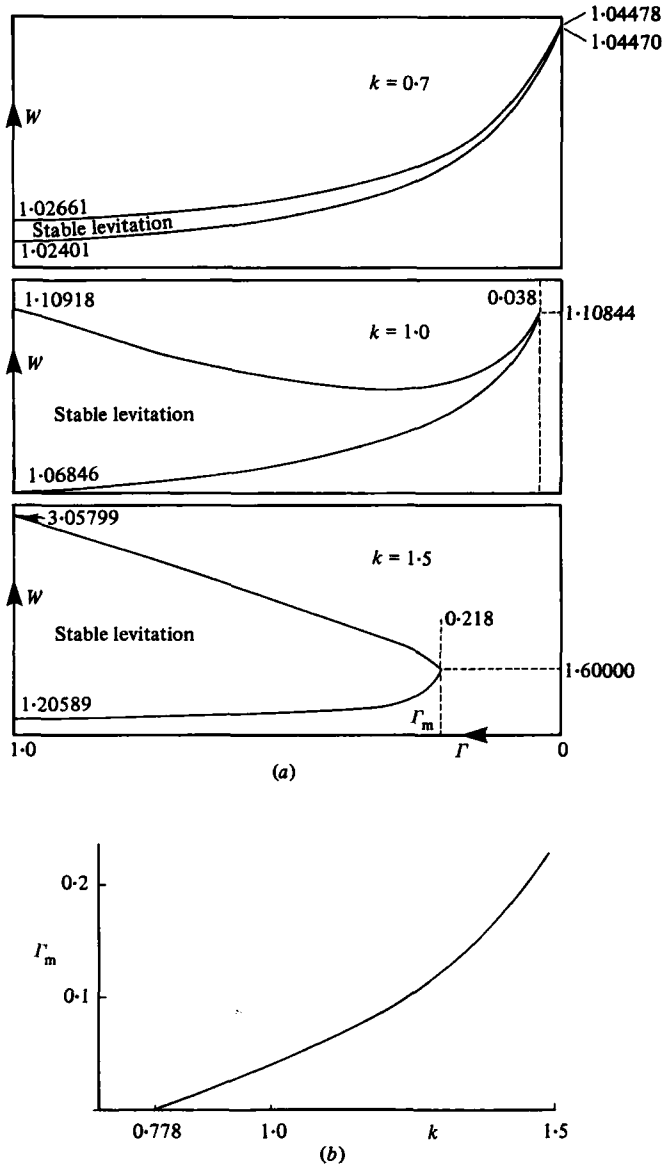


FIGURE 8. (a) Regions of stable levitation for  $k = 0.7, 1.0, 1.5$ . Note the different vertical scale in each diagram. (b) Graph of  $\Gamma_m(k)$ ; stable levitation is possible if  $\Gamma > \Gamma_m(k)$ .

### 6. Fluid motion in the levitated cylinder

In order to obtain some qualitative understanding of the motion within the cylinder, we shall ignore the departure of the cylinder cross-section from a circle (a procedure that is strictly justifiable only if surface tension is strong, i.e.  $\Gamma \gg 1$ ). From (3.14) the surface vorticity generation is, in the cylindrical geometry,  $\alpha^{-1} p_{M0} f'(\theta)$ , the function  $f(\theta)$  being as shown in figure 5, for various  $k$ . There are apparently two distinct possibilities: (i) if  $k$  is small,  $f(\theta)$  decreases monotonically from  $\theta = 0$  to  $\theta = \pi$ , so that the

sign of vorticity generation does not change in this interval; (ii) for larger  $k$ ,  $f(\theta)$  reaches a maximum at some intermediate point, where the vorticity generation therefore changes sign. One would expect the resulting fluid motion to consist of two eddies in case (i), and four in case (ii), as is in fact found (see figure 9 below, which shows only the right-hand half of the flow domain).

We have argued in §2 that the flow is likely to be turbulent when  $L \sim 10$  mm and greater, and that a uniform eddy viscosity  $\nu_T \sim u_0 L$  may then provide the dominant mechanism of momentum transfer. The Reynolds number based on  $\nu_T$  is of order unity, and a *low* Reynolds number analysis is likely to give a reasonable qualitative description of the mean flow. This, at any rate, is the approach we now adopt.†

The streamfunction  $\psi(r, \theta)$  of the mean flow then satisfies the (inhomogeneous) bi-harmonic equation

$$\nabla^4 \psi = -\frac{1}{\rho \nu_T} (\nabla \wedge \bar{\mathbf{F}})_z = -\frac{2p_{M0}}{a\rho \nu_T \delta} \exp\left\{-\frac{2(a-r)}{\delta}\right\} f'(\theta). \quad (6.1)$$

The circle  $r = a$  is a streamline on which the tangential stress vanishes, and so

$$\psi = 0, \quad \frac{\partial^2 \psi}{\partial r^2} - \frac{1}{r} \frac{\partial \psi}{\partial r} = 0 \quad \text{on} \quad r = a. \quad (6.2)$$

Now the right-hand side of (6.1) is significant only within the magnetic boundary layer, within which  $\nabla^4 \approx \partial^4/\partial r^4$ , and so a particular integral of (6.1) is

$$\psi_1 = \frac{p_{M0} \delta^3}{8a\rho \nu_T} \exp\left\{-\frac{2(a-r)}{\delta}\right\} f'(\theta), \quad (6.3)$$

the general solution (with appropriate symmetry) being

$$\psi = \psi_1 + \sum_{n=1}^{\infty} \left( A_n \left(\frac{r}{a}\right)^n + B_n \left(\frac{r}{a}\right)^{n+2} \right) \sin n\theta. \quad (6.4)$$

The boundary conditions (6.2) then determine the coefficients  $A_n$  and  $B_n$ , in terms of the Fourier coefficients  $f_n$  of  $f(\theta)$  (see 5.17). Retaining only leading order terms in the small parameter  $\delta/a$ , the solution for  $(a-r)/\delta \gg 1$  is

$$\psi = \frac{p_{M0} a \delta}{8\rho \nu_T} (1-R^2) \sum_{n=1}^{\infty} f_n R^n \sin n\theta, \quad (6.5)$$

where  $R = r/a$ .

The series in (6.5) may actually be summed! To do this, consider first the complex conjugate series

$$E(R, \theta) = \frac{1}{2} f_0 + \sum_{n=1}^{\infty} f_n R^n \cos n\theta \quad (6.6)$$

for which, from (5.19) and (3.11),

$$E(1, \theta) = f(\theta) = (l^2 - a^2)^2 (r_1^{-2} + r_2^{-2}). \quad (6.7)$$

It can be shown by elementary trigonometry that on the circle  $r = a$ ,

$$(l^2 - a^2) r_i^{-2} = 2l r_i^{-1} \cos \theta_i - 1 \quad (i = 1, 2), \quad (6.8)$$

† This is to be contrasted with the approach of Mestel (1982) who uses numerical methods to determine the corresponding laminar flow in a sphere at *high* Reynolds number.

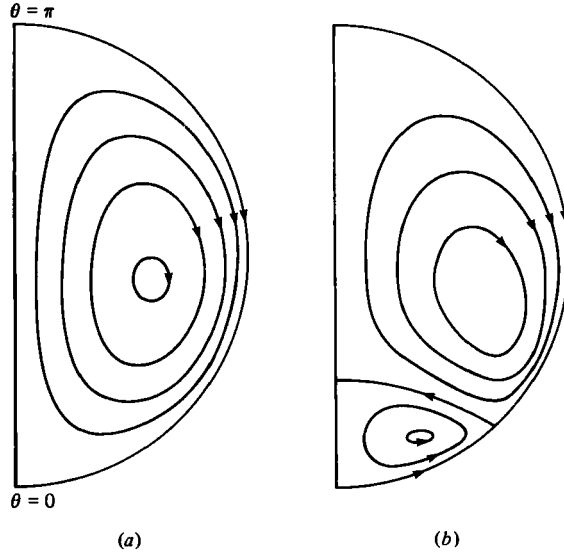


FIGURE 9. Streamlines  $\psi = \text{cst.}$  where  $\psi$  is given by the low Reynolds number solution (6.13); (a)  $k = 0.5, \eta = 1.1$ ; (b)  $k = 0.95, \eta = 1.0$ .

where  $r_i, \theta_i$  are defined in figure 4b, and that

$$\frac{\cos \theta_1 \cos \theta_2}{r_1 r_2} = C_0 + C_1 \left( \frac{\cos \theta_1}{r_1} + \frac{\cos \theta_2}{r_2} \right) + C_2 \frac{\cos (\theta_1 + \theta_2)}{r_1 r_2}, \quad (6.9)$$

where

$$\left. \begin{aligned} C_0 &= -(l^2 - a^2 \cos 2\alpha)/C_4, & C_1 &= l(l^2 + a^2 - 2a^2 \cos 2\alpha)/C_4, \\ C_2 &= (l^2 - a^2)^2/C_4, & C_4 &= 2(l^4 + a^4 - 2a^2 l^2 \cos 2\alpha). \end{aligned} \right\} \quad (6.10)$$

Substitution of (6.8) and (6.9) in (6.7) gives

$$\begin{aligned} E(1, \theta) &= 2l^2 \left( \frac{\cos 2\theta_1}{r_1^2} + \frac{\cos 2\theta_2}{r_2^2} \right) + D_1 \left( \frac{\cos \theta_1}{r_1} + \frac{\cos \theta_2}{r_2} \right) + D_2 \frac{\cos (\theta_1 + \theta_2)}{r_1 r_2} + D_0 \\ &= V(r_1, r_2, \theta_1, \theta_2), \quad \text{say,} \end{aligned} \quad (6.11)$$

where

$$\left. \begin{aligned} D_1 &= 8l(C_1 l - 1) + 4l^3/(l^2 - a^2), & D_2 &= 8l^2 C_2, \\ D_0 &= 4 + 8l^2 C_0 - 4l^2/(l^2 - a^2). \end{aligned} \right\} \quad (6.12)$$

Since  $E(R, \theta)$  and  $V$  are both harmonic in  $R < 1$  and equal on  $R = 1$ , they must be equal throughout  $R < 1$ . The complex conjugate of (6.11) is obtained by replacing cosines by sines; hence (6.5) may be written

$$\begin{aligned} \psi = \frac{p_{M0} a \delta}{8\rho\nu_T} (1 - R^2) \left[ 2l^2 \left( \frac{\sin 2\theta_1}{r_1^2} + \frac{\sin 2\theta_2}{r_2^2} \right) + D_1 \left( \frac{\sin \theta_1}{r_1} + \frac{\sin \theta_2}{r_2} \right) \right. \\ \left. + D_2 \frac{\sin (\theta_1 + \theta_2)}{r_1 r_2} + D_0 \right]. \end{aligned} \quad (6.13)$$

Figure 9 shows streamline patterns for two values of  $(k, \eta)$ , which have the structure anticipated from the argument based on the sign of vorticity generation. However,

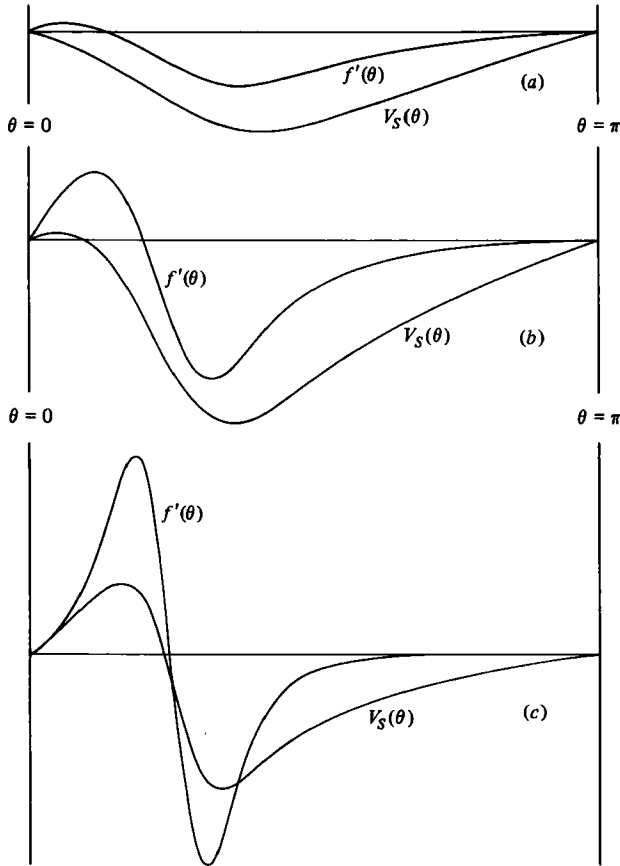


FIGURE 10. Graphs of  $f'(\theta)$  and the surface velocity  $V_S(\theta)$ : (a)  $k = 0.5$ ,  $\eta = 1.1$ ; (b)  $k = 0.75$ ,  $\eta = 1.2$ ; (c)  $k = 0.95$ ,  $\eta = 1.0$ . Note that the zero of  $V_S$  is displaced towards  $\theta = 0$ , relative to the zero of  $f'(\theta)$ .

the point at which the surface velocity

$$V_S = a^{-1}(\partial\psi/\partial R)_{R=1}, \quad (6.14)$$

changes sign does not quite coincide with the point where  $f'(\theta) = 0$  (figure 10) but is slightly displaced towards  $\theta = 0$ .

## 7. Discussion

The results of §§ 3, 5 and 6 show the feasibility of levitating a two-dimensional liquid metal cylinder in the magnetic field due to parallel line currents in phase, which can be thought of as representing in cross-section a fluid torus levitated by two circular line currents (figure 2a). This geometry avoids the crucial difficulty associated with practical levitation devices, viz that surface tension is necessary to prevent fluid from leaking through the lower neutral magnetic-field point; and indeed we have found that levitation is possible with zero surface tension, and that there is (in principle) no limit to the mass of liquid metal that can be levitated with a sufficiently high current. An

immediate qualification is however appropriate: although this system can be made stable with respect to perturbations in the plane of cross-section, it would be subject to longitudinal instabilities due to surface tension (which would tend to divide the torus into drops) and due to the tendency of the torus to sink lower into the magnetic field at any point where the cross-sectional area was increased by longitudinal inflow. Nevertheless such instabilities could be eliminated by the application of a sufficiently strong longitudinal magnetic field – the same technique that is used to eliminate the plasma pinch instability – and a toroidal levitation device could probably be made to work.

There are however a number of obvious imperfections in the analysis that we have been able to develop. Firstly, the shape calculation was based on the variational principle (5.10) which is valid only if dynamic pressure effects are negligible. A complete solution of the problem clearly requires inclusion of dynamic pressure in (5.1) and this requires solution of the dynamical problem within a free surface that is strongly distorted by magnetic pressure – a formidable problem even if the flow were known to be laminar. Secondly, accepting that the flow is likely to be turbulent, there is the problem of improving significantly on the assumption of uniform eddy viscosity, adopted in §6. A similar problem of turbulence modelling in flows with closed streamlines driven by rotational forces arises in related contexts (see, for example, Hunt & Maxey 1980), but we appear to be still far from an adequate solution. Of course, the normal component of fluctuating velocity falls to nearly zero (exactly zero if surface ripples are ignored) at the free surface, and so a decrease in eddy viscosity near the free surface is to be expected. This effect should perhaps be incorporated in a more realistic analysis.

Finally, there are questions of global stability associated with the fact that in practice it is voltage, rather than current, that is generally prescribed in the external coils. Perturbations in the shape of the levitated sample lead to an associated perturbation in the mutual inductance between coils and sample, and so to the possibility of dynamic instability involving this coupling.

All of these effects require further analysis in conjunction with experiments aimed at providing some detailed information concerning the velocity field within the sample and on its surface.

This work was initiated at the School of Mathematics, University of Bristol, in 1978/9 during A.D.S.'s tenure of an S.R.C. Senior Visiting Fellowship, Grant no. GR/B 04969. Professor M. R. Harris of the University of Newcastle-upon-Tyne drew our attention to the comprehensive study of Stephan (1975), and provided helpful criticism and comments which are gratefully acknowledged.

#### REFERENCES

- BLOCK, F. R. & THEISSEN, A. 1971 Electromagnetic levitation melting – method of crucible-free melting. *Elektrowärme Int.* **29**, 349.
- BRANCHER, J. P. & SERO GUILLAUME, O. 1981 Sur l'équilibre des ferrofluides avec interface libre. Rapport interne, LEMTA, Nancy, France.
- BRISLEY, W. & THORNTON, B. S. 1963 Electromagnetic levitation calculations for axially symmetric systems. *Brit. J. Appl. Phys.* **14**, 682.
- EL-KADDAH, N. H. & ROBERTSON, D. C. C. 1978 The kinetics of Gas-Liquid metal reactions involving levitated drops. *Metall. Trans.* **9B**, 191.

- HARRIS, M. R. & STEPHAN, S. Y. 1975 Support of liquid metal surface by alternating magnetic field. *IEEE Trans. MAG-11*, 1508.
- HATCH, A. J. 1965 Potential-well description of electromagnetic levitation. *J. Appl. Phys.* **36**, 44.
- HUNT, J. C. R. & MAXEY, M. R. 1980 Estimating velocities and shear stresses in turbulent flows of liquid metals driven by low frequency electromagnetic fields. In *MHD Flows and Turbulence*, (ed. H. Branover & A. Yakhot), Israel Universities Press, Jerusalem.
- LIGHTHILL, M. J. & WHITHAM, G. B. 1955 On kinematic waves. I. Flood movement in long rivers. *Proc. Roy. Soc. A*, **229**, 281.
- MESTEL, J. 1982 Magnetic levitation of liquid metals. *J. Fluid Mech.* **117**, 27.
- MOREAU, R. 1980 Applications métallurgiques de la magnétohydrodynamique. In *Proc. XVth Int. Cong. Theor. Appl. Mech.* (ed. F. P. J. Rimrott & B. Tabarrok), North Holland.
- MUCK, O. 1923 German Pat. No. 422004, Oct. 30 1923.
- OKRESS, E. O., WROUGHTON, D. M., COMENETZ, C., BRACE, P. N. & KELLY, J. C. K. 1952 Electromagnetic levitation of solid and molten metals. *J. Appl. Phys.* **23**, 83.
- PEIFER, W. A. 1965 Levitation melting, a survey of the state-of-the-art, *J. Metals* **17**, 487.
- PIGGOT, L. S. & NIX, G. F. 1966 Electromagnetic levitation of a conducting cylinder. *Proc. I.E.E.* **113**, 1229.
- SMITHELLS, C. J. 1967 *Metals Reference Book* 4th. edn. vols. I and III, Butterworths, London.
- SNEYD, A. D. 1979 Fluid flow induced by a rapidly alternating or rotating magnetic field. *J. Fluid Mech.* **92**, 35.
- STEPHAN, S. Y. 1975 Support of liquid metal surfaces by alternating magnetic fields - an experimental and theoretical study. Ph.D. thesis, University College, London.
- VOLKOV, T. F. 1962 Stability of a heavy conducting fluid contained by a rapidly varying magnetic field. *Soviet Phys. - Tech. Phys.*, **7**, 22.
- ZHEZHERIN, T. F. 1959 Problems of magnetohydrodynamics and plasma dynamics. *Izv. AN Latv. SSR. Riga.* **279**.